Replacement of Tyrosine D with Phenylalanine Affects the Normal Proton Transfer Pathways for the Reduction of $P680^+$ in Oxygen-Evolving Photosystem II Particles from *Chlamydomonas*

C. Jeans,[‡,§] M. J. Schilstra,[‡,||] N. Ray,[⊥] S. Husain,[⊥] J. Minagawa,[#] J. H. A. Nugent,[⊥] and D. R. Klug*[,‡]

Molecular Dynamics Group, Department of Chemistry, Imperial College, London SW7 2AY, United Kingdom, Department of Biology, Darwin Building, University College London, Gower Street, London WC1E 6BT, United Kingdom, and Photodynamics Research Centre, RIKEN, 19-1399 Koeji, Aoba, Sendai 980-0868, Japan

Received August 27, 2002

ABSTRACT: We have probed the electrostatics of $P680^+$ reduction in oxygenic photosynthesis using histidine-tagged and histidine-tagged Y_D-less Photosystem II cores. We make two main observations: (i) that His-tagged *Chlamydomonas* cores show kinetics which are essentially identical to those of Photosystem II enriched thylakoid membranes from spinach; (ii) that the microsecond kinetics, previously shown to be proton/hydrogen transfer limited [Schilstra et al. (1998) *Biochemistry 37*, 3974−3981], are significantly different in Y_D-less *Chlamydomonas* particles when compared with both the His-tagged *Chlamydomonas* particles and the spinach membranes. The oscillatory nature of the kinetics in both *Chlamydomonas* samples is normal, indicating that S-state cycling is unaffected by either the histidine-tagging or the replacement of tyrosine D with phenylalanine. We propose that the effects on the proton-coupled electron transfers of $P680^+$ reduction in the absence of Y_D are likely to be due to p*K* shifts of residues in a hydrogen-bonded network of amino acids in the vicinity of Y_Z. Tyrosine D is 35 Å from Y_Z and yet has a significant influence on proton-coupled electron transfer events in the vicinity of Y_Z. This finding emphasizes the delicacy of the proton balance that Photosystem II has to achieve during the water splitting process.

Photosystem II (PSII)[1] is the membrane−protein complex which catalyses electron transfer from water to plastoquinone (*1*−*3*). In PSII, electron transfer starts with the excitation of the reaction center chlorophyll *a*, P680, to its excited form P680* and rapid electron transfer away from P680*, via pheophytin, to the bound plastoquinone, Q_A, to form the $P680^+Q_A^-$ state. Subsequent electron transfer then occurs from Q_A^- to a second plastoquinone, Q_B. Following two turnovers, Q_B has accepted two electrons and taken up two protons. Q_BH_2 dissociates from its site into the membrane pool of plastoquinone and is replaced by a new molecule of Q_B. $P680^+$ extracts an electron from the water-oxidizing complex (WOC) via tyrosine-161 (cyanobacterial numbering) on the polypeptide D1 (PSII-A) commonly known as Y_Z. Sequential electron extraction cycles the WOC through oxidation states of the Mn cluster (named S_0 to S_4). During the S-state cycle, two molecules of water bind to the OEC (*4*). During the S_3 to S_0 transition, the S_4 state is transiently formed, which spontaneously decays to S_0, releasing one molecule of O_2. In the dark, the S_2 and S_3 states decay to S_1 within a few minutes. On further dark adaptation, the S_0 state is oxidized to S_1 by a second redox-active tyrosine, Y_D, tyrosine-160 on the D2 (PSII-D) polypeptide (*5*−*7*). Evidence indicates that D2 histidine-190 forms a hydrogen bond to Y_D, which is located in a relatively hydrophobic pocket (*8*−*10*).

The kinetics of reduction of $P680^+$ by Y_Z and subsequently $Y_Z^\bullet$ (the neutral radical) by the WOC are dependent on the S-state. A large fraction of $P680^+$ is reduced by Y_Z in nanoseconds, but at least 15% occurs on time scales smaller than 1 μs (*11*−*17*). In a previous paper (*15*), we investigated the reduction kinetics of $P680^+$ during the S-state transitions. Our analysis concentrated on differences between decays within a series of flashes, by subtracting the averaged decay from the individual curves, so that contributions of nonoscillatory processes disappear. These results showed that the S-state-dependent oscillatory behavior extended from the nanosecond domain far into the microsecond domain. We also found that there is no significant deuterium isotope effect on processes that occur in the nanosecond time domain, but that H_2O/D_2O exchange causes a significant decrease in the $P680^+$ reduction rate in the microsecond time domain. This

* To whom correspondence should be addressed. Tel/Fax: (44) 020 7594 5806. E-mail: d.klug@ic.ac.uk.

‡ Imperial College.

§ Current address: Biochemistry Department, Bristol University, Bristol BS8 1TD, United Kingdom.

|| Current address: Biocomputation group, Science and Technology Research Centre, University of Hertfordshire, College Lane, Hatfield, Hertfordshire, AL10 9AB, United Kingdom.

⊥ University College London.

Photodynamics Research Centre.

[1] Abbreviations: PSI, Photosystem I; PSII, Photosystem II; C-PSII, histidine-tagged PSII particles from wild-type *Chlamydomonas*; C-PSII-Y_D^-, histidine-tagged PSII particles from a tyrosine D-less mutant D2-Y160F of *Chlamydomonas*; BBY, granal stack membrane preparation from spinach; Y_Z, tyrosine-161 on the D1 polypeptide of PSII (*Synechocystis* numbering); Y_D, tyrosine-160 on the D2 polypeptide of PSII (*Synechocystis* numbering); P680, chlorophyll *a* primary electron donor in PSII; P700, chlorophyll *a* primary electron donor in PSI; EPR, electron paramagnetic resonance; DCBQ, 2,6-dichlorobenzoquinone; fwhm, full width at half-maximum.

10.1021/bi020558e CCC: $22.00
Published on Web 12/07/2002

suggests a role for proton-coupled electron transfer processes, in which proton/hydrogen transfer is required to complete the reduction of $P680^+$ through an alteration in the equilibrium between $Y_Z/Y_Z^\bullet$ and $P680/P680^+$. These results have been confirmed by other researchers (*16*, *18*).

Lifetimes of <3 to 250 μs have been reported for the transition $Y_Z^\bullet S_0/Y_Z S_1$, 30−140 μs for $Y_Z^\bullet S_1/Y_Z S_2$, 100−600 μs for $Y_Z^\bullet S_2/Y_Z S_3$, and up to 4.5 ms for $Y_Z^\bullet S_3/Y_Z S_0$ (*19*, *20*). Four protons are released to the lumenal side of the thylakoid membrane during the S-state cycle. This release of protons into the lumen, together with proton uptake at the stromal Q_B site, creates a pH gradient across the membrane. The stoichiometry of the proton release is dependent on the pH and on the preparation of PSII used. The release of the four protons is distributed more or less equally over the four light-induced transitions (S_0/S_1 to S_3/S_0) in the S-state cycle (reviewed in ref *21*) for core complexes. Evidence has been presented that the proton release into the bulk takes place within some tens of microseconds after the excitation (*19*, *22*). This means that proton release precedes the actual S-state transition and is coupled to $P680^+$ reduction and Y_Z oxidation, rather than to Y_Z reduction and the oxidation of water itself.

The green unicellular alga *Chlamydomonas reinhardtii* is a eukaryotic model system for studies of photosynthesis. *Chlamydomonas* can be transformed and has the ability to grow heterotrophically using acetate while still synthesizing the photosynthetic apparatus, so that a range of photosynthetic mutants can be made. However, the biochemical and biophysical analysis of PSII in *Chlamydomonas* has been hindered by the difficulties of purifying PSII while retaining activities such as water oxidation. Recently the use of metal affinity chromatography has been used to purify PSII from *Chlamydomonas* (*23*, *24*). The procedure uses mutants in which a number of histidine residues have been added to a PSII polypeptide using molecular genetics. We have produced a novel histidine-tagged PSII using a rapid purification procedure, which produces from *C. reinhardtii* a PSII preparation free of PSI that retains very high activities such as oxygen evolution. In this paper, we present an investigation of the reduction kinetics of $P680^+$ during the four S-state transitions in PSII preparations from histidine-tagged native PSII and histidine-tagged mutant D2-Y160F PSII.

MATERIALS AND METHODS

Strains and Culture Conditions. *C. reinhardtii* cells were grown in Tris−acetate phosphate (TAP) medium or high salt minimal (HSM) (*25*) at 25 °C under an illumination of 10−20 (small cultures) or 20−100 (8L cultures) μE m^{-2} s^{-1} photosynthetically active radiation. Chlorophyll assays were performed on cells and PSII according to the methods of Arnon (*26*) and Porra (*27*).

Construction of the Histidine-Tagged PSII-H Mutant. Recombinant DNA techniques were according to standard protocols (*28*). The histidine-tagged PSII-H was constructed and was used to transform a *psb*H disruption mutant, H-null opposite, of *C. reinhardtii* (*29*). This disruption mutant was constructed using insertion of the *aad*A antibiotic resistance cassette within the *psb*H gene. Transformation was carried out using the biolistic technique as in ref *29*. Transformants were selected for by recovery of photoautotrophic growth, as the PSII-H-deficient mutant lacks PSII and therefore is unable to grow photoautotrophically. This process also leads to loss of the *aad*A antibiotic resistance cassette. Transformants, termed H-his, were taken through more than three rounds of single colony isolations on HSM to obtain homoplasmic lines. This was confirmed by Southern blot analysis of miniprep DNA (*28*) and by PCR. Incorporation of the histidine tag was confirmed by oligonucleotide sequencing of the transformant *psb*H gene (ABI Prism 377). This gave a translated C-terminal amino acid sequence for PSII-H of LAKVSQLHHHHHH for H-his PSII-H compared to LAKVS for wild-type PSII-H.

Isolation of PSII from the C. reinhardtii H-His Mutant. Throughout the purification procedure, cells and PSII were exposed to minimum light and were kept at 4 °C. *C. reinhardtii* cells were harvested, washed, and then broken in a French press. The membranes were solubilized at a concentration of 1 mg Chl/mL with 25 mM dodecyl maltoside (DM) at pH 6.5 and centrifuged at 11 000*g* for 10 min to remove debris. Protease inhibitors (Sigma) were added as a precaution. The supernatant was added to washed nickel resin (Qiagen) in 25 mM MES (pH 6.5), 100 mM NaCl, 10% glycerol, 0.03% (w/v) DM, 10 mM ascorbic acid, and 5 mM imidazole. After 30 min, the slurry was poured into a chromatography column and washed until the eluate was clear. The PSII was eluted with buffer as above but at pH 6.0 and containing 200 mM imidazole and then mixed with an equal volume of 20 mM MES (pH 6.3), 15 mM NaCl, 20%(w/v) poly(ethylene glycol) (PEG) 3000, 10 mM ascorbic acid, and 10 mM EDTA. The precipitate was pelleted by centrifugation at 11 000*g* for 10 min. The pellet was resuspended in 20 mM MES (pH 6.3), 15 mM NaCl, 10 mM ascorbic acid, 10% PEG 3000 or 8000, 10 mM $CaCl_2$ and centrifuged again at 11 000*g* for 10 min. The PSII was finally resuspended and stored in a small volume of 20 mM MES (pH 6.3), 15 mM NaCl, 333 mM sucrose, and 10 mM $CaCl_2$ (Final buffer). Manganese depletion of *C. reinhardtii* PSII was achieved by incubating PSII at 0.5 mg/mL and 275 K in Final buffer excluding $CaCl_2$ but containing 10 mM NH_2OH for 10 min. The samples were pelleted and washed using a repeat of the PEG precipitation steps above and resuspended in Final buffer.

Construction of Histidine-Tagged PSII-D2-Y160F Mutant. The C-PSII-Y_D^- was constructed by introducing a site-directed mutation, D2-Y160F, into a His-tagged *psb*D plasmid, pBD3020H, which is similar to pBD110H (*23*) but has a recyclable *aad*A cassette (*30*) in the middle of the *psa*A2 gene so as to inhibit the expression of the *psa*A gene. The D2-Y160F mutation was introduced by a "Mega-primer" method (*31*) using the mutagenic oligonucleotide, 5′-TTC-CTAATTTTCCCATTAGGT-3′. Incorporation of the tyrosine to phenylalanine change was confirmed by oligonucleotide sequencing of the transformant *psb*D gene.

Electron Paramagnetic Resonance (EPR) Analysis. For EPR, 0.3−0.4 mL samples (approximately 1−3 mg Chl/mL) were placed in calibrated ~3 mm quartz EPR tubes. Identical sets of samples in calibrated EPR tubes were made for each experiment, using the same preparation and chlorophyll concentration. They were given a brief (*30s*) illumination at 277 K to turnover the PSII reaction center and restore $Y_D^\bullet$ lost on storage. They were then dark adapted for 1 h and then frozen in liquid nitrogen in the dark. Samples were

illuminated at 200 K using an ethanol/dry ice bath in an unsilvered clear glass dewar and a 1000 W light source, protecting the sample from heating by a 5 cm water filter, before storage at 77 K in liquid nitrogen in the dark.

Samples were examined by EPR at cryogenic temperatures using a JEOL RE1X X-band spectrometer (9.090 GHz) with 100-kHz modulation and fitted with an Oxford Instruments cryostat. EPR conditions are given in the figure legends. Illumination in the EPR cavity was by a 150 W light source and fiberoptic light guide. Spectra were recorded and manipulated using a Dell microcomputer running Asyst software. No filtering, smoothing, fitting, or background subtractions were used. The vertical scale showing first derivative EPR spectra is arbitrary, with spectra at the same instrument gain. The field scale corresponds to *g*-values as follows: $g = 6$ at 108 mT, $g = 3$ at 216 mT, and $g = 2$ at 323 mT.

Isolation of PSII from Spinach. Oxygen-evolving PSII-enriched granal membranes (BBYs) were prepared from fresh market spinach according to ref *32*, with the minor modifications described in ref *19*. The membrane fragments were stored at −80 °C at a chlorophyll concentration of 5 mg/mL in a buffer containing 25 mM MES pH 6.5, 10 mM NaCl, 5 mM $MgCl_2$, 5 mM $CaCl_2$, and 0.3 M sucrose (SMNCB). Manganese depletion of BBY membranes was achieved by incubating membranes at 5 mg chlorophyll/mL at room temperature in SMNCB containing 50 mM NH_2OH for 5 min. The membranes were pelleted in an eppendorf centrifuge (5 min at 15 000 rpm) and washed once with SMNCB before use.

Oxygen Evolution Analysis. Steady-state oxygen evolution studies were performed using a Clark type oxygen electrode. The electron acceptors used were 2,6-dimethylbenzoquinone (final concentration 1 mM) and potassium ferricyanide (final concentration 1 mM). Average values and standard deviations from triplicate measurements for each were 1900 ± 160 μmol O_2 (mg Chl)$^{-1}$ h^{-1} for C-PSII and 2000 ± 200 μmol O_2 (mg Chl)$^{-1}$ h^{-1} for C-PSII-Y_D^-. The O_2 evolution rate of the BBY preparation was approximately 800 μmol O_2 (mg Chl)$^{-1}$ h^{-1} when 2,6-dichlorobenzoquinone (DCBQ) was used as a secondary acceptor. DCBQ was purchased from Kodak and dissolved in ethanol (96%) to a concentration of 50 mM. All measurements were carried out at saturating illumination; this was checked by routinely measuring rates at different chlorophyll concentrations. Mn-depleted particles showed <5% the oxygen evolution rates of the corresponding intact particles.

Transient Absorption Spectroscopy. The equipment used has been described in detail previously (*15*). In short, the samples were excited by saturating flashes from a frequency doubled, Q-switched Nd:YAG laser ($\lambda = 532$ nm, pulse duration 7 ns (fwhm), 10 mJ/ pulse, corresponding to 20 mJ cm^{-2} at the sample). $P680^+$ reduction was monitored at 830 nm, using a 35 mW continuous wave laser diode as a light source. Scattered excitation light and fluorescence were excluded by an appropriate combination of spatial and transmission filters. The response time of the system was 10 ns (fwhm). The signals were transferred to a 100 MHz oscilloscope (Gould 4072, 400 Ms/s, or Tektronix TDS 220, 1 Gs/s), and from there via an IEEE 488 instrumentation interface to a PC. Samples were diluted in SMNCB to final concentrations of 20 (*C. reinhardtii* preparations) or 80 (BBYs) μg/mL of chlorophyll, to which 0.015% (w/v) dodecyl maltoside (*C. reinhardtii* preparations) or 0.016% (w/v) Triton X-100 (BBYs) was added to reduce the light scattering caused by large aggregates. The samples (250 μL) were placed in a 4 mm × 4 mm fluorescence cuvette. Under these conditions, the transmission of the samples was about 80% (BBYs and C-PSII-Y_D^-) or 50% (C-PSII), although there was some variation between batches. The lower transmission in the C-PSII sample does not reflect inhomogeneity in this sample, merely a differing level of aggregation. Addition of higher concentrations of dodecyl maltoside improved the transmission to a degree. However, to avoid the potential for altered kinetics at very high detergent concentrations, we chose to work at this lower transmission: minimizing docecyl maltoside concentration but maintaining sufficient transmission to obtain good signal/noise. We know that aggregation does not affect the kinetics, and this is confirmed by the data presented here.

Immediately prior to the measurements, 100 μM DCBQ was added. The curves shown in Figures 3−5 are the average of 100 excitations, and to produce the data in Figure 6, 20 (BBYs), 40 (C-PSII), or 170 (C-PSII-Y_D^-) data sets of 21 consecutive excitations each were averaged. Global and autocorrelation analyses were carried out as described in (*15*), and miss factors were estimated using the equations derived by (*33*).

RESULTS

EPR Measurements. To confirm that the isolated PSII was suitable for biophysical analysis, EPR measurements were performed. Using EPR spectroscopy it is possible to establish the PSI and PSII content of thylakoids or PSII preparations using observations on characteristic spectra from their electron transfer components; for example, the spectrum of $Y_D^\bullet$ in dark adapted samples is indicative of PSII, whereas the $P700^+$ spectrum, formed on illumination at cryogenic temperatures, is indicative of PSI. EPR can detect these components at low levels, and hence it is an extremely sensitive diagnostic tool. In Figure 1 the $Y_D^\bullet$ spectrum present in dark adapted samples in wild-type *C. reinhardtii* (Figure 1A, bold line) is absent in the H-null mutant that lacks PSII (Figure 1B) but is present in the histidine-tagged transformant (Figure 1C) and the PSII isolated from it (C-PSII, Figure 1D, bold line). Following illumination at 12 K, the signal for the $P700^+$ is present in the wild-type (Figure 1A, outer line), the H-null (Figure 1B, bold outer line), and histidine-tagged mutant (Figure 1C, outer line). The purified histidine-tagged PSII (C-PSII, Figure 1D) does not show the signal for $P700^+$, confirming the absence of PSI. The small increase on illumination of the C-PSII (Figure 1D, outer line) is mostly due to oxidation of Y_D reduced during storage at 77 K before the EPR experiment and partly to formation of Chl^+ (Chl Z^+) (*34*−*36*) in PSII, which can be distinguished from $P700^+$ by its broader line width. No signal from the PSI iron−sulfur center A or B was detected by EPR (not shown) confirming that this small increase was not due to any (>1%) residual PSI.

To confirm that all Y_D had been removed in the histidine-tagged Y_D-less *Chlamydomonas* strain (C-PSII-Y_D^-), the spectra of purified PSII from C-PSII and C-PSII-Y_D^- were compared. Figure 2 shows spectra from PSII particles isolated

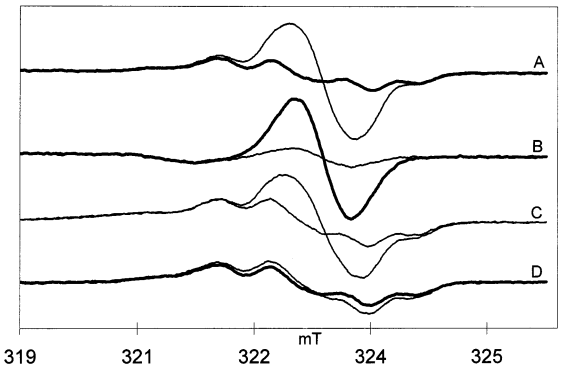

FIGURE 1: EPR spectra showing the purification of PSII in the histidine-tagged transformant of *C. reinhardtii*. In each pair of spectra, the inner line is the spectrum of a dark adapted sample, whereas the outer line is the spectrum following illumination for 2.5 min at 12 K. (A) Wild-type thylakoid membranes. The bold inner line shows the spectrum of $Y_D^{\bullet}$. (B) H-null thylakoid membranes. The bold outer line shows the $P700^+$ induced by illumination. (C) Thylakoid membranes from the histidine-tagged transformant. (D) Purified PSII from the histidine-tagged transformant (C-PSII) showing the absence of $P700^+$ after illumination. EPR conditions: microwave power 0.001 mW, modulation amplitude 0.2 mT, temperature 12 K.

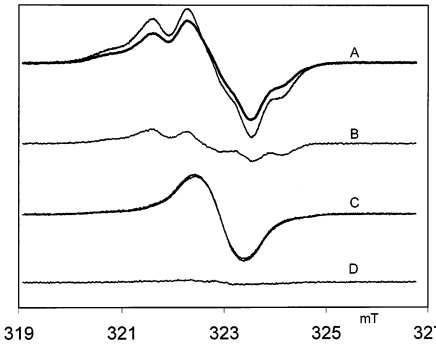

FIGURE 2: EPR spectra of purified PSII from histidine-tagged (C-PSII, 2.9 mg Chl/mL) and D2-Y160F/histidine-tagged (C-PSII-Y_D^-, 2 mg Chl/mL) *C. reinhardtii* strains. Samples were illuminated at 200K, stored at 77 K for 1 week, and then re-illuminated in the cavity at 10 K. The $Y_D^{\bullet}$ spectrum is clearly seen in the dark adapted C-PSII but is not present in the spectrum for C-PSII-Y_D^-. (A) C-PSII before and after reillumination at 10 K. (B) Illuminated minus stored dark difference spectrum from sample A showing spectrum of $Y_D^{\bullet}$ restored by illumination. (C) C-PSII-Y_D^- before and after reillumination at 10 K showing the absence of $Y_D^{\bullet}$. The spectrum in the C-PSII-Y_D^- sample is probably Chl Z^+ or Car^+ (see text for further detail). (D) Illuminated minus stored dark difference spectrum from sample C. EPR conditions: microwave power 0.001 mW, temperature 10K, modulation amplitude 0.2 mT.

from C-PSII, (Figure 2A) and C-PSII-Y_D^- (Figure 2C). Samples were illuminated at 200 K to fully oxidize Y_D. During subsequent storage at 77 K, a slow (i.e., days) recombination of electron acceptor $Qa^{\bullet -}$ with $Y_D^{\bullet}$ occurs in some centers (*34*−*36*). Each sample was stored at 77 K for 1 week; the resulting spectrum was recorded then the sample was re-illuminated in the EPR cavity at 10 K and the spectrum recorded again. After illumination the signal from $Y_D^{\bullet}$ (shown by the difference spectrum Figure 2B) in C-PSII is fully restored, but no $Y_D^{\bullet}$ is seen in C-PSII-Y_D^- (Figure 2D) as expected. The signal seen in C-PSII-Y_D^- is probably from oxidized carotenoid, Car^+, and/or the accessory chlorophyll, Chl Z^+, these components acting as secondary electron donors to PSII (*34*−*36*). The spectra confirm the absence of the redox-active tyrosine, Y_D, in the C-PSII-Y_D^-

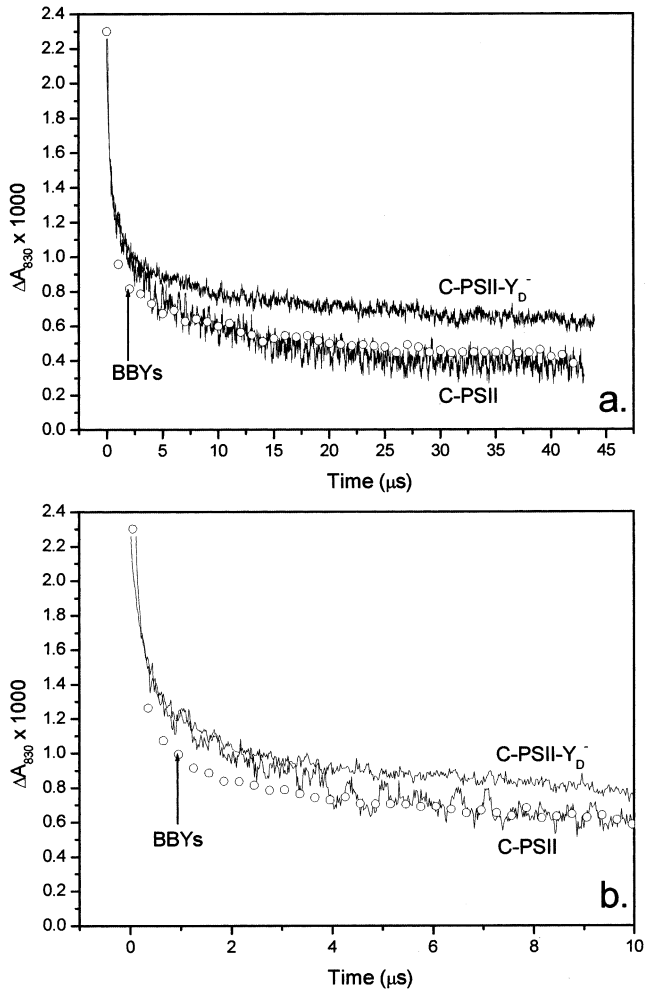

FIGURE 3: Average $P680^+$ reduction kinetics in His-tagged PSII (C-PSII) and His-tagged Y_D-less PSII (C-PSII-Y_D^-) from *Chlamydomonas* compared with BBYs. (a) Kinetics in all three preparations on a 40 μs time scale. The upper line represents C-PSII-Y_D^-, and the lower line represents C-PSII. $P680^+$ reduction kinetics in BBYs (○) are shown at one point per microsecond for clarity. Curves are the average of 100 excitations, collected at 20 ns/channel. (b) Closeup of the first 10 μs of panel a. For clarity, the BBY data (○) are shown at one point per 300 ns. See Table 1 for the results of exponential fits to these data.

and also that its absence disturbs the pathways of electron donation to $P680^+$ at cryogenic temperatures, allowing secondary donors to be detected more easily.

$P680^+$ Reduction Kinetics. The average $P680^+$ reduction kinetics were measured for PSII particles isolated from a His-tagged D2-Y160F mutant of *Chlamydomonas* (C-PSII-Y_D^-), a control His-tagged *Chlamydomonas* strain (C-PSII), and PSII membranes from spinach (BBYs). These are shown in Figure 3. The BBY data were normalized to give the same initial $P680^+$ concentration as the C-PSII and C-PSII-Y_D^- data. The normalization factor indicated that the C-PSII and C-PSII-Y_D^- particles both contain about 40 molecules of chlorophyll per P680, assuming about 250 molecules of chlorophyll per P680 in BBYs and similar PSII membrane preparations (*32*, *37*, *38*). The slight difference between the $P680^+$ reduction kinetics in the BBY and C-PSII preparations may be due to small differences in the fraction of particles lacking the oxygen-evolving complex. Importantly though, the kinetics in C-PSII and C-PSII-Y_D^- are indistinguishable for the first few microseconds. After this, the reduction

Table 1: Results of Multiexponential Fits to Data Shown in Figure 3[a]

sample	τ_1 (ns) ± S.E.	A_1 (%)	τ_2 (ns) ± S.E.	A_2 (%)	τ_3 (μs) ± S.E.	A_3 (%)	τ_4 (μs) ± S.E.	A_4 (%)	A_5 (%)
C-PSII	14 ± 3	37	150 ± 30	25	0.7 ± 0.1	11	8 ± 0.4	19	8
C-PSII-Y_D^-	15 ± 3	38	190 ± 20	28	1.8 ± 0.1	14	15 ± 0.8	7	13
BBYs	18 ± 4	26	110 ± 10	33	0.7 ± 0.1	18	12 ± 1.6	12	11

[a] Data over 50 μs were fitted to a sum of four exponentials and an offset. Lifetimes are quoted with standard errors derived from the fitting procedure. Amplitudes are expressed as percentages of the total amplitude. Standard errors in the amplitudes are less than 10% of the quoted percentage. χ-square values for the fits are as follows: C-PSII, 5×10^{-4} (4×10^{-3} for 3 exponentials and an offset); C-PSII-Y_D^-, 8×10^{-4} (2×10^{-3} for 3 exponentials and an offset); BBYs, 8×10^{-5} (6×10^{-4} for 3 exponentials and an offset).

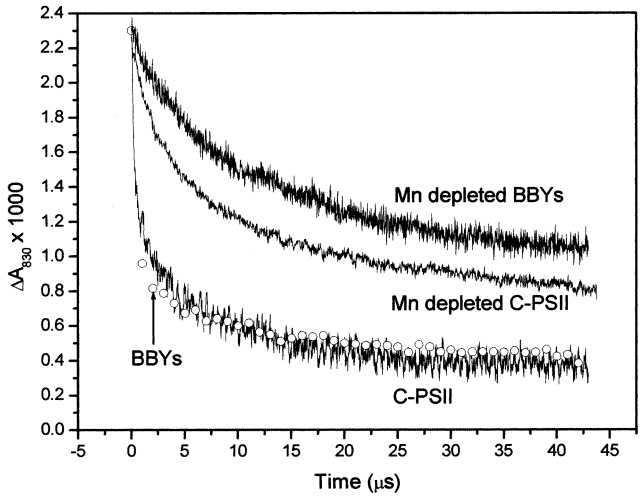

FIGURE 4: Average $P680^+$ reduction kinetics in BBYs (○, shown at one point per microsecond for clarity), Mn-depleted BBYs, C-PSII, and Mn-depleted C-PSII. Mn depletion was carried out by washing the samples in buffer containing hydroxylamine (see Materials and Methods). Curves are the average of 100 excitations, collected at 20 ns/channel.

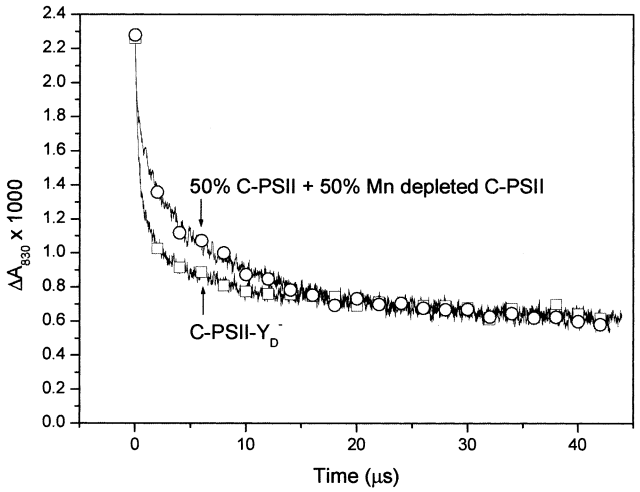

FIGURE 5: $P680^+$ reduction kinetics in C-PSII-Y_D^- (□) and in a simulated linear combination of 50% C-PSII and 50% Mn-depleted C-PSII (○). This graph shows that the altered microsecond kinetics in C-PSII-Y_D^- cannot be due to the presence of a larger fraction of Mn-depleted particles in that preparation. Data for C-PSII-Y_D^- were taken from Figure 3, and data for the linear combination were calculated from the C-PSII and Mn-depleted C-PSII in Figure 4.

kinetics in C-PSII-Y_D^- are slow compared to both C-PSII and BBYs.

To quantify these visible differences in kinetics, the *Chlamydomonas* data shown in Figure 3 were fitted to multiexponential decays. A sum of four exponentials and an offset were required to adequately describe the data over 50 μs. The results of these fits are shown in Table 1. The parameters which describe the kinetics in C-PSII agree well with those for BBYs. In C-PSII-Y_D^- the lifetime τ_3 (and to a lesser extent τ_2) is significantly longer than that in the control preparations. There is significant variation in the microsecond lifetime τ_4 between the three samples, probably since this lifetime is long compared to the time scale of the data and is therefore difficult to determine accurately. However, in C-PSII-Y_D^- it can be seen that the offset A_5 makes up an increased proportion of the microsecond kinetics with respect to A_4, indicating the presence of components of longer lifetimes which cannot be determined from 50 μs of data. This fitting protocol therefore confirms in a quantitative manner the conclusion drawn from Figure 3 that only the microsecond phases are affected by the replacement of Y_D with phenylalanine.

Manganese-depleted C-PSII samples were also examined. The main purpose of checking these kinetics was to ensure that the differences observed in the microsecond time domain in C-PSII-Y_D^- could not be explained by a larger proportion of Mn-depleted particles in that preparation. A typical decay is shown in Figure 4, along with those of intact C-PSII and both intact and Mn-depleted BBYs. The kinetics are slowed in Mn-depleted C-PSII, in agreement with the situation in Mn-depleted BBYs (*39*). One obvious explanation of the data might be that the C-PSII-Y_D^- particles have a higher proportion of Mn-depleted particles. Figure 5 shows the average $P680^+$ reduction kinetics of C-PSII-Y_D^- compared with a simulated decay which is a linear combination of 50% C-PSII and 50% Mn-depleted C-PSII. This combination only fits the C-PSII-Y_D^- data after approximately 15 μs: before this time, the combination predicts a much slower rate of $P680^+$ reduction. This means that the altered microsecond kinetics in C-PSII-Y_D^- cannot be explained by the presence of Mn-depleted particles: no proportion will be able to fit both the microsecond phases and the sub-microsecond ones.

To compare kinetics from active particles, the deviations from the average $P680^+$ reduction kinetics due to S-state cycling over 21 consecutive flashes were analyzed (see *15* for a justification). These oscillatory deviations from average over 2.5 μs were fitted and required a sum of three exponentials and an offset to give a random distribution of residuals. The data from all three particles were fitted together, and the lifetimes were linked, since varying them independently did not significantly improve the fit. The lifetimes obtained were 20, 130, and 600 ns, and the amplitudes are plotted in Figure 6. The period-4 oscillatory kinetics are almost identical in all three particles, as are the miss factors: 12% for BBYs, 10% for C-PSII, and 13% for C-PSII-Y_D^-. The miss factor is the probability that an actinic flash will not result in S-state advancement and is responsible for the damping of the oscillations shown in Figure 6. The 20 ns component (A_1, maximal in flashes 1, 4, and 5) relates

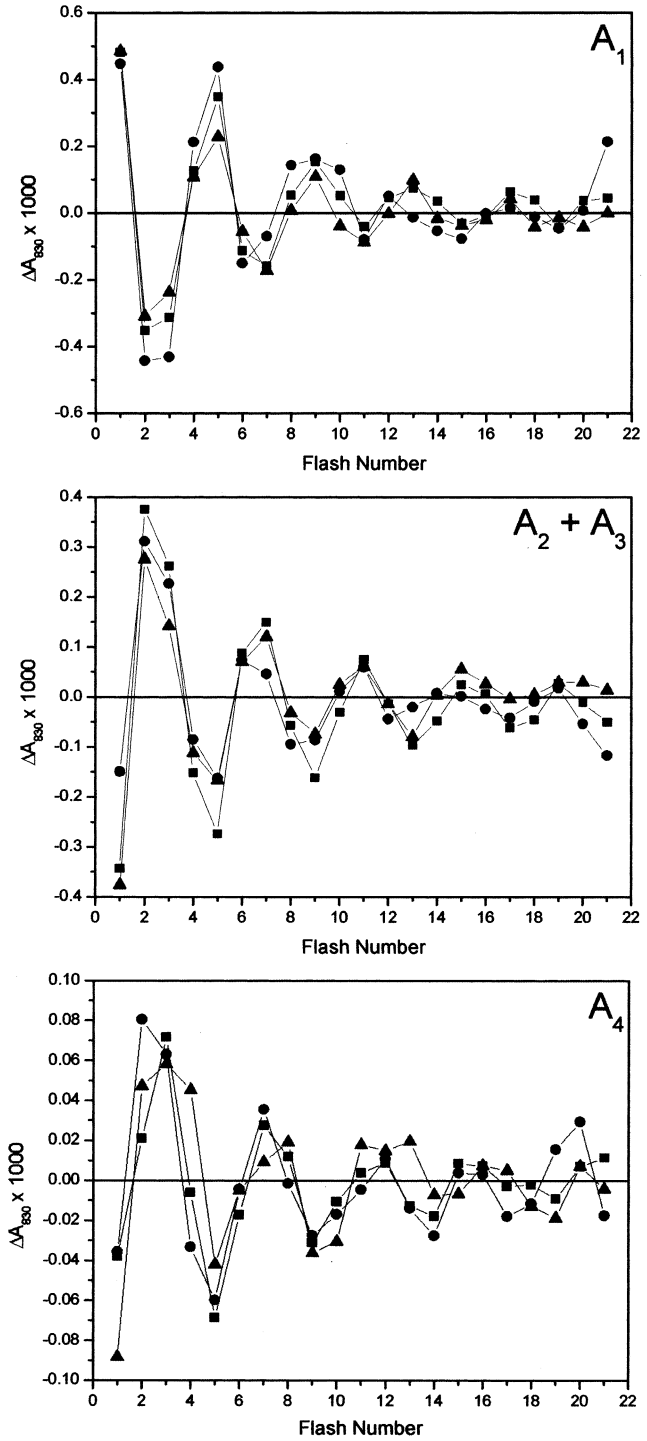

FIGURE 6: Oscillations in the kinetic components of $P680^+$ reduction in BBYs (■), C-PSII (●), and C-PSII-Y_D^- (▲) over 21 flashes. Difference from mean data on a 2.5 μs time scale were fitted to a sum of three exponentials and an offset. The lifetimes obtained were 20, 130, and 600 ns. Amplitudes A_1, $A_2 + A_3$, and A_4 (offset) are plotted here. The composite amplitude $A_2 + A_3$ is plotted due to the strong correlation between these two components (see *15*).

mainly, but not exclusively, to events occurring in the S_0 to S_1 and S_1 to S_2 transitions. The 130 ns and 600 ns components (A_2 and A_3, maximal in flashes 2 and 3) relate largely to the S_2 to S_3 and S_3 to S_0 transitions. There was a strong correlation between A_2 and A_3 in all data sets (see also *15*), and therefore, only the composite $A_2 + A_3$ is presented here.

DISCUSSION

General. The average kinetics of $P680^+$ reduction in PsbH histidine-tagged PSII from *Chlamydomonas* are very similar to those of PSII from spinach (Figure 3), with slightly faster kinetics over the first few microseconds. As the kinetics in C-PSII-Y_D^- are identical to those of C-PSII for the first few microseconds, it is likely that this slight difference with BBYs in this time domain is a real feature of the *Chlamydomonas* system. The pattern of oscillations in C-PSII are, however, indistinguishable from that in BBYs (Figure 6). Histidine-tagged PSII from *Chlamydomonas* seems therefore to be a suitable model PSII preparation and a suitable control for the experiments described in this paper.

Beyond 2−3 μs, the kinetics in C-PSII-Y_D^- are slowed compared to both C-PSII and BBYs. This cannot be explained by an increased proportion of Mn-depleted particles in the C-PSII-Y_D^- preparation, as demonstrated in Figure 5. It is clear from Figure 3 that the equilibrium constant for the microsecond phases of $P680^+$ reduction has been altered by the mutation. This will affect both the observed rate constant (since for a shallow equilibrium, the observed rate is the sum of the forward and backward rates) and the amplitudes of the kinetic components. It is not possible at this stage to determine how much of the observed change is due to rate constant changes and how much is due to amplitude changes, since the two are interlinked. From the observation that the amplitudes of the oscillations are the same in all particles (Figure 6), it seems reasonable to conclude that the amplitudes are likely to have been affected far less by the mutation than the rate constants and that the main effect of the D2-Y160F mutation has been to slow the rates of electron transfer in the microsecond domain. The kinetics in the microsecond domain have been shown by H_2O/D_2O exchange experiments to be rate limited by proton/hydrogen transfer (*15*, *16*, *18*). Proton/hydrogen transfer is suggested to be required to complete $P680^+$ reduction through a shift in the equilibrium between Y_Z and $P680^+$. In light of this, the simplest interpretation of the results presented here is that the replacement of Y_D with phenylalanine perturbs the normal proton transfer pathways which occur during $P680^+$ reduction. The electron transfers which are not rate limited by proton transfer seem totally unaffected, since the kinetics of C-PSII-Y_D^- before 2−3 μs are indistinguishable from those of C-PSII. At first glance, it is difficult to rationalize this retardation of proton transfer with structural knowledge of PSII. Tyrosine D is approximately 35 Å from Y_Z (*40*) and about the same distance from the manganese cluster (*41*, see also models in refs *42*−*44*) and is normally assumed to have no role in water splitting. It is hydrogen bonded through its phenolic proton to a histidine residue, D2-His190 (*8*, *9*, *42*, *45*). Although the proton involved in the motions in the microsecond phases of $P680^+$ reduction has not been identified, it seems likely that it is one in the chain of the hydrogen-bonded amino acids on D1 in the region of Y_Z (*17*, *46*−*49*). How Y_D could affect motions on this side of PSII is not immediately obvious.

The results presented here suggest that Y_D affects the proton/hydrogen transfers which accompany the relaxation phases of $P680^+$ reduction. This does not necessarily mean that Y_D is directly involved in a proton transfer pathway, but merely that its electrostatic or structural contribution is

required for normal proton/hydrogen transfer. Its absence is likely to cause shifts in the p*K*s of nearby amino acid side chains. Previous work on a Y_D-less mutant of *Synechocystis* showed that the structure or redox properties of Y_Z were altered (*50*), so this kind of 'action at a distance' is not unprecedented.

It has previously been suggested that $Y_D^\bullet$, present in the light, is partially responsible for pushing the $P680^+$ cation over to the Y_Z side of PSII (see *51*) in order to increase the rate of Y_Z to $P680^+$ electron transfer compared to Y_D to $P680^+$. It might therefore be expected that in the absence of Y_D, the P680/$P680^+$ redox potential would be affected. We see no evidence for this. Even a small change in the free energy gap between P680 and Y_Z should be noticeable in the average rate of $P680^+$ reduction, causing either an increase or a decrease in the rate constants for all of the sub-microsecond phases. This follows from electron transfer theory relating the rate of electron transfer to the free energy gap (and hence the redox potential difference) between the two redox components (*52*). (As the microsecond phases are rate limited by proton transfers, nonadiabatic electron transfer theory is irrelevant for these phases). Figure 3 clearly shows that only the microsecond phases have been affected by the D2-Y160F mutation. More quantitatively, Table 1 shows that while τ_1 is unchanged in C-PSII-Y_D^- compared to C-PSII and BBYs, τ_2 is marginally slowed and τ_3 is significantly slowed. Only if all sub-microsecond phases were seen to slow or speed up in response to the D2-Y160F mutation, would it be possible to correlate this to a shift in the redox potential of P680.

A recent paper has described the effects of the D2-Y160F mutation in *Synechocystis* on assembly of the Mn cluster (*53*). This showed that assembly of the cluster occurred more slowly and with a lower quantum efficiency in the mutant compared to wild-type. They considered that one possible explanation for the observed effects was that $Y_D^\bullet$ acts to raise the redox potential of $P680^+$/P680 by about 20 meV (*53*). However, this value was calculated using earlier data showing the $P680^+/Q_A^-$ recombination rate to be altered in Mn-depleted particles of this mutant (*50*). How applicable the data from the Mn-depleted system are to a system undergoing assembly of the Mn cluster is not clear. Using an equation derived by Dutton (*54*) to predict the effect of free energy changes on the electron transfer rate, we estimate that a shift of about 20 meV in the redox potential of $P680^+$/P680 would be observable as an alteration of the sub-microsecond kinetics; such an alteration is not observed. Further work to investigate the possibility of a small change in redox potential including close study of the fastest (20 ns) phases of $P680^+$ reduction in C-PSII-Y_D^- will clarify this issue.

Period-4 Oscillations. The oscillatory kinetics in all three preparations are essentially identical (Figure 6). The lifetimes and oscillation patterns obtained from the analysis in this report are similar to those reported previously (*15*). The observation that the C-PSII sample shows normal oscillations indicates that the histidine-tagging used here in no way impairs the S-state cycle; this is confirmed by the high rates of oxygen evolution obtained. Similarly, the mutation of Y_D to phenylalanine does not affect S-state cycling.

It is not currently known how much of the microsecond kinetics of $P680^+$ reduction are due to relaxations of the equilibrium constant and how much are due to inhomogeneity within the sample. De Wijn et al. proposed that deprotonation of D1-His190 is rate limiting for the microsecond phases of $P680^+$ reduction in 11−12% of particles, implying heterogeneity in the protonation state of this residue in the sample (*55*). However, they emphasized the difficulties in distinguishing between heterogeneity and relaxation of equilibria (*55*). A dynamic heterogeneity has been proposed (*56*) in which there is a redistribution of effective and ineffective stabilizers of charge separation on a 10 ms time scale. This too is difficult to distinguish experimentally from the equilibrium relaxation model proposed by Rappaport et al. (*57*). Nevertheless, it is generally agreed upon that the microsecond phases of $P680^+$ reduction reflects events occurring in water-splitting centers and that they involve proton/hydrogen motions (*15*, *16*). We can therefore look at the effects of the D2-Y160F mutation on these phases regardless of their actual origin.

The observation that the amplitude of the microsecond oscillations is the same in all three particles is worthy of note. It suggests that the effect of the D2-Y160F mutation is independent of the S-state, and lends support to the proposal that the main effect of the mutation is on the rates of electron transfer in the microsecond time domain. It further supports the conclusion that the altered microsecond kinetics in the C-PSII-Y_D^- sample are not due to a larger proportion of Mn-depleted particles, since an increased number of non-oxygen-evolving centers would result in diminished oscillations in the microsecond phase.

It is known that S_0 reacts with $Y_D^\bullet$ to form the S_1 state (*5*, *7*), this being an important reaction in the dark adaptation process, converting a 25% S_0 and 75% S_1 sample to 100% S_1 over a period of hours. It is not possible to tell whether this dark adaptation is occurring in the mutant sample, since under the conditions of the experiments reported here (YAG repetition rate 1 Hz) it is not possible to distinguish between 75% initial S_1 and 100% initial S_1 (*5* and references therein).

Tyrosine D can be oxidized by the manganese cluster in S_2 and S_3 only, this process being pH dependent and having a lifetime of 1−30 s (*58*). The $Y_D^\bullet$ radical can be reduced by the S_0 state of the manganese cluster, with a pH dependent lifetime of 5−40 min (*5*, *7*). In comparison, the $Y_Z^\bullet$ radical is reduced by all S-states, with lifetimes from around 3 μs to 4.5 ms (see Introduction). The $Y_D^\bullet/Y_D$ couple is thought to have a redox potential of around 750 mV (*7*), whereas the $Y_Z^\bullet/Y_Z$ couple probably has a redox potential of about 1 V (*59*). It has been suggested that Y_D may be involved in the photoactivation process, donating electrons to $P680^+$ to minimize possible photodamage caused by this oxidant in the absence of a functioning manganese cluster (*5*, *60*). It has also been proposed to be involved in stabilizing the intact cluster through its reaction with the S_0 state, in which manganese is thought to be more weakly bound (*5*, *61*). Our results show that normal S-state cycling occurs in C-PSII-Y_D^- (Figure 6), although the average $P680^+$ reduction kinetics are altered (Figure 3). It is possible that the purification procedure discriminates against PSII centers with incomplete Mn clusters, and so it is not possible for us to conclude anything categoric about the role of Y_D in photoassembly. In PSII with fully assembled Mn clusters however, replacement of Y_D with phenylalanine has a clear effect on the proton-limited electron transfer steps.

Conclusions. We have shown that the D2-Y160F mutation has no effect on the oscillatory nature of $P680^+$ reduction but that it has selectively affected the proton-limited electron transfers, which occur with a microsecond rate constant. We see no evidence for a change in the free energy gap between P680 and Y_Z, which implies that, at least for the sub-microsecond phases, the presence of $Y_D^\bullet$ does not affect the redox potential of $P680/P680^+$. The most likely cause of the altered microsecond kinetics in the mutant are shifts in the p*K*s of residues in a hydrogen-bonded network in and around the Y_Z site. Such shifts could easily be produced by the absence of the phenolic proton of Y_D, which is known to be closely associated with Y_D in both its oxidized and reduced states.

REFERENCES

1. Diner, B. A., and Babcock, G. T. (1996) in *Oxygenic Photosynthesis: The Light Reactions* (Ort, D. R., and Yocum, C. F., Eds.) pp 213−247, Kluwer Academic Publishers, Dordrecht, The Netherlands.
2. Britt, R. D. (1996) in *Oxygenic Photosynthesis: The Light Reactions* (Ort, D. R., and Yocum, C. F., Eds.) pp 137−164, Kluwer Academic Publishers, Dordrecht, The Netherlands.
3. Nugent, J. H. A. (1996) *Eur. J. Biochem. 237*, 519−531.
4. Hillier, W., and Wydrzynski, T. (2001) *Biochim. Biophys. Acta 1503*, 197−209.
5. Styring, S., and Rutherford, A. W. (1987) *Biochemistry 26*, 2401−2405.
6. Vass, I., Deak, Z., and Hindeg, E. (1990) *Biochim. Biophys. Acta 1017*, 63−69.
7. Vass, I., and Styring, S. (1991) *Biochemistry 30*, 830−839.
8. Tang, X.-S., Chisholm, D., Dismukes, G., Brudvig, G., and Diner, B. (1993) *Biochemistry 32*, 13742−13748.
9. Tommos, C., Davidsson, L., Svensson, B., Madsen, C., Vermaas, W., and Styring, S. (1993) *Biochemistry 32*, 5436−5441.
10. Tommos, C., Madsen, C., Styring, S., and Vermaas, W. (1994) *Biochemistry 33*, 11805−11813.
11. Brettel, K., Schlodder, E., and Witt, H. T. (1984) *Biochim. Biophys. Acta 766*, 403−415.
12. Schlodder, E., Brettel, K., Schatz, G. H., and Witt, H. T. (1984) *Biochim. Biophys. Acta 765*, 178−185.
13. Meyer, B., Schlodder, E., Dekker, J., and Witt, H. (1989) *Biochim. Biophys. Acta 974*, 36−43.
14. Lukins, P. B., Post, A., Walker, P. J., and Larkum, A. W. D. (1996) *Photosynth. Res. 49*, 209−221.
15. Schilstra, M. J., Rappaport, F., Nugent, J. H. A., Barnett, C. J., and Klug, D. R. (1998) *Biochemistry 37*, 3974−3981.
16. Christen, G., Reifarth, F., and Renger, G. (1998) *FEBS Lett. 429*, 49−52.
17. Christen, G., Seeliger, A., and Renger, G. (1999) *Biochemistry 38*, 6082−6092.
18. Christen, G., and Renger, G. (1999) *Biochemistry 38*, 2068−2077.
19. Rappaport, F., Blanchard-Desce, M., and Lavergne, J. (1994) *Biochim. Biophys. Acta 1184*, 178−192.
20. Razeghifard, M., Klughammer, C., and Pace, R. (1997) *Biochemistry 36*, 86−92.
21. Lavergne, J., and Junge, W. (1993) *Photosynth. Res. 38*, 279−296.
22. Haumann, M., and Junge, W. (1994) *Biochemistry 33*, 864−872.
23. Sugiura, M., Inoue, Y., and Minagawa, J. (1998) *FEBS Lett. 426*, 140−144.
24. Sugiura, M., Minagawa, J., and Inoue, Y. (1999) *Plant Cell Physiol. 40*, 311−318.
25. Rochaix, J.-D., Mayfield, S., Goldschimdt-Clermont, M., and Erickson, J. (1988) in *Plant Molecular Biology: A Practical Approach* (Schaw, C.-H., Ed.) pp 253−275, IRL Press, Oxford.
26. Arnon, D. I. (1949) *Plant Physiol. 24*, 1−15.
27. Porra, R., Thompson, W., and Kriedmann, P. (1989) *Biochim. Biophys. Acta 975*, 384−394.
28. Sambrook, J., Frisch, E., and Maniatis, T. (1989) *Molecular Cloning. A Laboratory Manual*, 2nd ed., Cold Spring Harbor Press, New York.
29. O'Connor, H., Ruffle, S., Cain, A., Deak, Z., Vass, I., Nugent, J., and Purton, S. (1998) *Biochim. Biophys. Acta 1364*, 63−72.
30. Fischer, N., Stampacchia, O., Redding, K., and Rochaix, J.-D. (1996) *Mol. Gen. Genet. 251*, 373−387.
31. Landt, O., Grunert, H.-P., and Hahn, U. (1990) *Gene 96*, 125−128.
32. Berthold, D. A., Babcock, G. T., and Yocum, C. F. (1981) *FEBS Lett. 134*, 231−234.
33. Lavorel, J. (1978) *J. Theor. Biol. 57*, 171−185.
34. de Paula, J. C., Innes, J. B., and Brudvig, G. W. (1985) *Biochemistry 24*, 8114−8120.
35. Hanley, J., Deligiannakis, Y., Pascal, A., Faller, P., and Rutherford, A. W. (1999) *Biochemistry 38*, 8189−8195.
36. Tracewell, C. A., Cua, A., Stewart, D. H., Bocian, D. F., and Brudvig, G. W. (2001) *Biochemistry 40*, 193−203.
37. Lam, E., Baltimore, B., Ortiz, W., Chollar, S., Melis, A., and Malkin, R. (1983) *Biochim. Biophys. Acta 724*, 201−211.
38. Ford, R., and Evans, M. (1983) *FEBS Lett. 160*, 159−164.
39. Ahlbrink, R., Haumann, M., Cherepanov, D., Bogershausen, O., Mulkidjanian, A., and Junge, W. (1998) *Biochemistry 37*, 1131−1142.
40. Astashkin, A., Kodera, Y., and Kawamori, A. (1994) *Biochim. Biophys. Acta 1187*, 89−93.
41. Debus, R. J. (1992) *Biochim. Biophys. Acta 1102*, 269−352.
42. Svensson, B., Vass, I., Cedergren, E., and Styring, S. (1990) *EMBO J. 9*, 2051−2059.
43. Ruffle, S. V., Donnelly, D., Blundell, T. L., and Nugent, J. H. A. (1992) *Photosynth. Res. 34*, 287−300.
44. Svensson, B., Etchebest, C., Tuffery, P., van Kan, P., Smith, J., and Styring, S. (1996) *Biochemistry 35*, 14486-14502.
45. Kim, S., Liang, J., and Barry, B. (1997) *Proc. Natl. Acad. Sci. U.S.A. 94*, 14406−14411.
46. Hays, A.-M. A., Vassiliev, I. R., Golbeck, J. H., and Debus, R. J. (1998) *Biochemistry 37*, 11352−11365.
47. Haumann, M., Mulkidjanian, A., and Junge, W. (1999) *Biochemistry 38*, 1258−1267.
48. Hays, A.-M. A., Vassiliev, I. R., Golbeck, J. H., and Debus, R. J. (1999) *Biochemistry 38*, 11851−11865.
49. Tommos, C., and Babcock, G. T. (2000) *Biochim. Biophys. Acta 1458*, 199−219.
50. Boerner, R. J., Bixby, K. A., Nguyen, A. P., Noren, G. H., Debus, R. J., and Barry, B. A. (1993) *J. Biol. Chem. 268*, 1817−1823.
51. Nugent, J. H. A., Rich, A. M., and Evans, M. C. W. (2001) *Biochim. Biophys. Acta 1503*, 138−146.
52. Moser, C. C., and Dutton, P. L. (1996) in *Protein Electron Transfer* (Bendall, D. S., Ed.) pp 1−21, BIOS Scientific Publishers Ltd, Oxford.
53. Ananyev, G. M., Sakiyan, I., Diner, B. A., and Dismukes, G. C. (2002) *Biochemistry 41*, 974−980.
54. Page, C. C., Moser, C. C., Chen, X., and Dutton, P. L. (1999) *Nature 402*, 47−52.
55. de Wijn, R., Schrama, T., and van Gorkom, H. J. (2001) *Biochemistry 40*, 5821−5834.
56. Lavergne, J., and Rappaport, F. (1998) *Biochemistry 37*, 7899−7906.
57. Rappaport, F., Porter, G., Barber, J., Klug, D., and Lavergne, J. (1995) in *Photosynthesis: From Light to Biosphere* (Mathis, P., Ed.) pp 345−348, Kluwer Academic Publishers, Montpelier.
58. Babcock, G., and Sauer, K. (1973) *Biochim. Biophys. Acta 325*, 483−503.
59. Metz, J. G., Nixon, P. J., Rogner, M., Brudvig, G. W., and Diner, B. A. (1989) *Biochemistry 28*, 6960−6969.
60. Magnuson, A., Rova, M., Mamedov, F., Fredriksson, P.-O., and Styring, S. (1999) *Biochim. Biophys. Acta 1411*, 180−191.
61. Nugent, J. H. A., Demetriou, C., and Lockett, C. J. (1987) *Biochim. Biophys. Acta 894*, 534−542.

BI020558E